Sand-coated Iron Mold Casting of Wind Turbine Main Shaft Made of High Strength and Low Temperature Impact Resistance Ductile Iron

Xiao-jiang Xia^{1,2}, *Da Shu¹, Zhong-bin Wu², Dong-hong Wang¹, Jun Tang³, Yun-qing Sheng², Ying Xiu², Qian-hai Gong³

- 1. Shanghai Key Lab of Advanced High-temperature Materials and Precision Forming and State Key Lab of Metal Matrix Composites, School of Materials Science and Engineering, Shanghai Jiao Tong University, Shanghai 200240, China;
 - 2. Zhejiang Institute of Mechanical & Electrical Engineering Co., Ltd., Hangzhou 310002, Zhejiang, China.
 - 3. Zhejiang Jiali Wind Power Technology Co., Ltd., Hangzhou 310051, Zhejiang, China;

*Corresponding address: e-mail: dshu@sjtu.edu.cn

Abstract: This study explores the application of sand-coated iron mold casting combined with a new material design for producing large wind turbine main shafts. The objective was to improve the mechanical properties, including tensile strength, yield strength, and low-temperature toughness, while ensuring a cost-effective and efficient casting process. Experimental results showed that the use of sand-coated iron mold casting significantly enhanced the tensile strength and yield strength of the main shaft, with improvements exceeding 40 MPa compared to conventional materials. The mechanical properties were consistent across different axial cross-sections of the main shaft, demonstrating high uniformity in performance. The newly designed material, with optimized chemical composition, also met the low-temperature impact toughness requirements. The results indicate that the sand-coated iron mold casting process is a promising alternative to traditional resin sand casting, providing higher strength and better consistency for large-scale wind turbine main shafts.

Keywords: Wind turbine main shaft; sand-coated iron mold casting; casting process; material design; mechanical properties; shrinkage porosity.

1 Introduction

The wind turbine main shaft is a key component that connects the hub and gearbox of a wind turbine. It bears significant torque and axial loads. The shaft is installed at heights of tens to even hundreds of meters. In some regions, the working temperature ranges from -20°C to -40°C. Additionally, wind speed varies significantly during operation. Wind turbine components are required to last for at least 20 years without the need for replacement. If failure occurs, the replacement costs are extremely high. Moreover, the resulting downtime due to the inability to generate power leads to even greater losses [1]. Therefore, the material properties of wind turbine main shafts must meet stringent requirements, including both high strength and low-temperature toughness. The conventional manufacturing process for wind turbine main shafts is alloy forging. However, this process is characterized by high costs, heavy components, and low yield rates. At the same time, with the growing demand for lightweight wind turbine products and cost

reduction, more wind turbine manufacturers are opting for ductile iron to replace forged steel. They are using a casting-to-forging process to produce the main shafts, which helps reduce production costs and improve economic efficiency. According to recent statistics, cast main shafts accounted for about 14% of the wind turbine main shaft market in 2022.

Currently, there are two main materials used for casting shafts: QT400-18L and QT500-14, with their material performance specifications shown in Tab. 1. QT400-18L is a ferrite matrix ductile iron, a material with a relatively mature application that offers good low-temperature impact toughness. However, its strength is relatively low, resulting in a lower safety factor during strength verification. On the other hand, QT500-14 employs a high-silicon solid solution strengthening approach, which significantly enhances material strength, but at the expense of reduced low-temperature impact toughness. Due to the thick walls of the shaft (with an average wall thickness greater than 100 mm) and

significant variations in wall thickness across different areas, resin sand casting is commonly used in production. This process involves slower solidification and cooling rates, with greater mold shrinkage, which can lead to defects such as graphite distortion, shrinkage cavities, and porosity in thicker sections, ultimately affecting the product's performance. As a result, improving both the overall mechanical properties and internal quality of the castings has become a common goal for all wind turbine manufacturers.

Table 1. Specifications of conventional shaft materials

| | Casting | TS | VC | YS Elongatio | AkV (-20°C)/J | | |
|----------|--|------|-------------|--------------|---------------|---------|--|
| Grade | Thickness | (MPa | | | Single | Average | |
| | (mm) |) | (MPa) n (%) | Value | Value | | |
| QT400-18 | 60 <t≤200< td=""><td>360</td><td>220</td><td>12</td><td>7</td><td>10</td></t≤200<> | 360 | 220 | 12 | 7 | 10 | |
| AL | 00<1 <u><</u> 200 | 300 | 220 | 12 | , | 10 | |
| QT500-14 | 60 <t≤200< td=""><td>450</td><td>350</td><td>13</td><td>2</td><td>3</td></t≤200<> | 450 | 350 | 13 | 2 | 3 | |

The composition of ductile iron is close to the eutectic point, resulting in a wide liquid-solid two-phase region at the solidification front. When the austenite surrounding the graphite comes close to contact, the still-liquid metal is divided into discrete, disconnected pools, losing the ability to shrinkage-compensate, and taking on a mushy state. As a result, the shell of the ductile iron casting lacks sufficient rigidity for an extended period after pouring. The solidification expansion force generated when the eutectic colonies come into contact not only increases the gap between the austenite dendrites but also causes the relatively fragile shell of the casting to expand outward. This prevents the final solidifying part of the casting from receiving enough liquid metal to compensate for shrinkage, leading to the formation of shrinkage cavities [2].

Sand-coated iron mold coating refers to applying a thin layer of sand on the inner cavity of a metal mold (iron mold), and then using this sand-coated iron mold for pouring the casting. Compared to sand casting, the coating of sand is relatively thin during solidification. Additionally, the sand layer has a high thermal conductivity, and the iron mold possesses strong heat retention capabilities. As a result, the heat from the molten metal is quickly transferred to the iron mold, which causes the casting to cool rapidly, refining the grain structure and improving mechanical properties. Compared to metal mold casting, the sand coating on the surface of the iron mold forms a thin sand layer. By adjusting the appropriate thickness of this coating, the casting can avoid cooling too quickly, which could lead

to white cast iron formation. At the same time, the iron mold has almost no flexibility, and the sand coating applied to the iron mold undergoes quartz transformation and expansion upon heating. This expansion helps counteract the expansion force from the molten metal [3].

The sand-coated iron mold coating technology, introduced to China in 1974 by the Zhejiang Mechanical and Electrical Design Institute, has been successfully applied in the casting of cast iron parts such as crankshafts, camshafts, and valve bodies. These castings typically range from a few kilograms to several tons in weight. However, there have been few reports of its application in castings weighing over 10 tons. The author believes the limited use of this technology in large castings in the early stages can be attributed to the following reasons: (1) The sand-coated iron mold coating technology requires higher investment in molds, equipment, and the iron mold itself, whereas resin sand is less costly. For large castings with insufficient order volumes, the economic feasibility of using sand-coated iron mold coating technology is relatively low. (2) There are few specialized institutions that concurrently research both sand-coated iron mold coating processes and related equipment, leading to a lack of comprehensive studies on the application of this technology for large parts.

However, the solidification mechanism of ductile iron is consistent for both large and small castings, and the application of sand-coated iron mold coating technology for large castings is entirely feasible. For large castings, the sand-coated iron mold coating technology can be applied based on the casting's structure. By adjusting the thickness of the sand coating and the iron mold during solidification, the casting can be prevented from forming white iron, while the rapid cooling of the iron mold ensures that the casting solidifies and cools quickly. This also helps to refine the grain size and enhance the material's overall mechanical properties. Furthermore, since the iron mold has no flexibility, the expansion force generated by the graphite formation during the solidification of ductile iron is counteracted by the resistance of the iron mold. This helps mitigate the tendency for shrinkage porosity and shrinkage cavities in the casting.

Additionally, based on the principle of balanced solidification, for thick and large ductile iron castings, the slow shrinkage rate and the relatively earlier graphite expansion are beneficial in balancing the expansion and contraction forces. This helps to shift the equilibrium point, making it possible to achieve sandless casting of

ductile iron parts using the combined sand-coated iron mold coating technology.

2 Casting process design

A certain model of wind turbine main shaft weighs approximately 22 tons, with dimensions of 2700 mm × 2700 mm × 3500 mm. The thinnest part has a wall thickness of 65 mm, while the thickest part reaches 230 mm. The model is shown in Fig. 1. This project proposes the use of sand-coated iron mold technology, along with the development of a new material to improve the overall mechanical properties of the main shaft. The objective is to achieve low-temperature toughness comparable to or exceeding that of QT400-18AL, while increasing its strength by more than 10% compared to QT400-18AL. The specific performance requirements are outlined in Tab. 2.



Fig. 1: Model of the wind turbine main shaft

Table 2. Performance requirements of new material (Including cast test samples)

| Grade | Casting Thickness (mm) | TS (MPa) | YS (MPa) | Elongation (%) | AkV (Single Value | -20°C)/J Average Value |
|--------------|--|-------------|-------------|----------------|--------------------|------------------------------|
| New Alloy | 60 <t≤200< td=""><td>390</td><td>240</td><td>12</td><td>7</td><td>10</td></t≤200<> | 390 | 240 | 12 | 7 | 10 |

2.1 Gating system design

The main shaft has a structural design where one end features a large flange, and the other has a smaller diameter. The thickest walls are located at both ends, while the middle section has thinner walls. Using a horizontal pouring method would facilitate parting of the mold, but the core length in the middle would be too long and unsupported, relying only on the core heads at both ends for support. This can lead to bending deformation and difficulties in maintaining consistent wall thickness. Additionally, during pouring, the molten metal from both sides converges at the top, which may cause defects like porosity and slag inclusion.

To address these issues, a vertical pouring method is adopted, with the large flange facing downward and the small diameter end facing upward. The casting height is 3500mm, with a pouring riser of approximately 325cm. Due to the large size of the riser, a bottom-pour casting process is used. The molten metal is directed vertically through a central pouring channel and flows into external filtering devices via four circumferential horizontal channels. The filtered molten metal then enters the cavity through 16 evenly distributed inner pouring channels around the bottom flange, ensuring a smooth fill while allowing impurities to rise to the top surface.

An open pouring system is employed, with a cross-sectional area ratio of the pouring system set as S vertical:S horizontal: S inner = 1:1.5:4.2. Four evenly distributed risers are placed circumferentially at the top of the casting. The pouring process is shown in Fig. 2. Given the shaft's structure and operational convenience, a composite molding method using sand-coated iron mold and resin sand is chosen. The external contour of the product is formed with sand-coated iron mold, while the inner cavity and top risers are made with resin sand. All pouring systems are arranged in the resin sand, which facilitates the placement of ceramic tubes and allows for further optimization of the pouring system, while also leveraging the advantages of sand-coated iron mold casting technology.

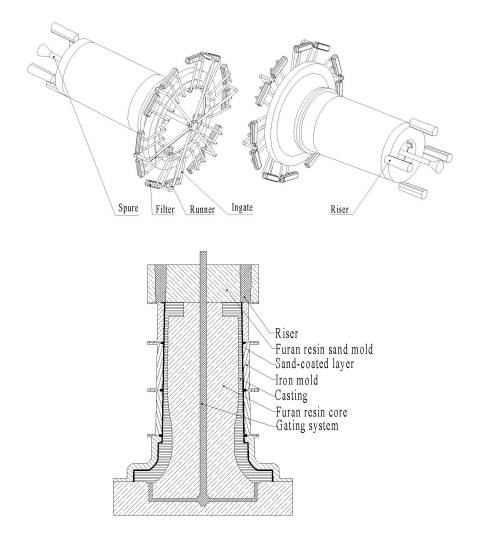


Fig. 2 : Schematic of the casting process

2.2 Casting Tooling Design

The wall thickness of the iron mold is determined based on the empirical formula (1):

tthick=
$$(0.6 \sim 0.8)$$
·tcasting [4] (1)

Where thick is the wall thickness of the iron mold (mm) and teasting is the wall thickness of the casting (mm).

The average wall thickness of the product is approximately 160 mm, with a coefficient of 0.6 applied. After minor adjustments based on the casting structure, the iron mold wall thickness is calculated to be 100 mm. The outer iron mold is divided into four sections, and to ensure the versatility of the sand shooting head, the basic shape of the iron mold is a uniform-walled cylindrical form. Both ends feature turning faces, and all dimensions of the iron mold are standardized. The internal cavity shape is designed to closely match the casting shape, with sand hanging grooves set at both ends for common mold closing and box alignment. Lifting shafts are positioned on the side. The iron mold structure is shown in Fig. 3. This casting has a ferritic matrix structure. Based on empirical data and considering the product dimensions, the sand covering layer is set to 15 mm. The iron mold model designed according to these specifications was verified, with the iron mold weight approximately 100 tons, 4.54 times the weight of the casting, which meets the empirical requirements.

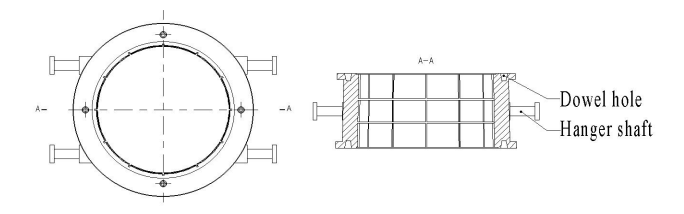


Fig. 3 : Schematic of iron mold model

To match the shape of the iron mold, the sand shooting head is designed to correspond with the turning face dimensions of the iron mold. The top section is equipped with sand inlets, an air reservoir, and a sand shooting control device. The sand shooting plate is designed with two concentric sealing rings. During sand shooting, the coated sand enters the mold cavity formed between the mold and the iron mold through the sand shooting holes between the two sealing rings. The process of iron mold coating is shown in Fig. 4.

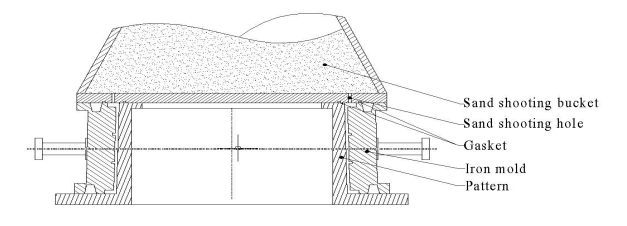


Fig. 4: Schematic of iron mold coating process

2.3 Material Composition Design

Sand-coated iron mold casting significantly differs from

sand mold casting, as the iron mold lacks flexibility, and its cooling rate during solidification is much faster, leading to greater supercooling compared to sand molds. Therefore, material composition must be tailored to the product structure casting process. Bv comprehensively analyzing the roles of various elements, considering the availability of raw materials both domestically and internationally, and drawing on experience data for producing QT400-18AL (-40 °C) low-temperature impact-resistant castings, the appropriate chemical composition range the production material is determined.

Silicon (Si) is an element that promotes graphitization, raising the eutectic temperature and reducing the eutectic carbon content. For low-manganese ferritic ductile cast iron, increasing Si content significantly lowers the impact toughness. Si also raises the brittle-to-ductile transition temperature of ductile iron ^[5]. To meet the low-temperature impact toughness requirements for the main shaft material, the Si content must be reduced. However, this leads to a decrease in material strength, making it difficult to meet the strength requirements. Therefore, to ensure toughness, the Si content is controlled within the range of 2.05% to 2.15%. At the same time, the strength deficit caused by reducing Si is addressed by enhancing the dual effects of graphitization elements and strengthening matrix elements.

Carbon equivalent has a significant impact on the fluidity of ductile iron. Increasing the carbon equivalent improves the fluidity of the alloy. Simultaneously, as the carbon equivalent increases, the volume of shrinkage cavities changes. When the carbon equivalent is between 4.2% and 4.8%, shrinkage porosity and shrinkage defects are minimized, resulting in sound castings. Carbon is a strong promoter of graphitization, and increasing carbon content reduces the shrinkage cavity volume and shrinkage porosity, leading to a denser casting. However, excessive carbon content can cause graphite floating. The carbon equivalent is primarily determined by the contents of C and Si. Since the Si content has already been set, and considering the strength reduction caused by lowering Si, the carbon equivalent is controlled at around 4.3%. The carbon content after spheroidization is maintained between 3.5% and 3.8%.

Manganese (Mn) is an element that expands the γ -phase region. While Fe and Mn completely dissolve in the liquid state, Mn exhibits a significant segregation tendency during solidification, accumulating at grain boundaries and promoting the formation of carbides. At

the same time, Mn negatively impacts the impact toughness and brittle-to-ductile transition temperature of ductile iron. To improve the material's toughness, Mn content must be minimized. According to the research of I. Riposan et al. ^[6], to achieve as-cast ferritic structure, Mn content should not exceed 0.2%. Due to the rapid cooling effect of the iron mold, the tendency for white cast formation increases compared to resin sand, so Mn content needs to be kept even lower. Considering the availability of raw materials, Mn content is controlled to be under 0.15%.

Phosphorus (P) is a harmful element in ductile iron, which deteriorates the material's mechanical properties. Sulfur (S) is a degraphitizing element and also a harmful impurity. S readily combines with rare earth elements and Mg in the nodulizing agent, consuming the nodulizer and causing nodulization degradation. Therefore, raw materials with low P and S content should be selected, with P content controlled to below 0.03% and S content not exceeding 0.02%.

Magnesium (Mg) is the primary nodulizing element in ductile iron. To ensure proper graphite nodulization, the alloy must contain a certain amount of residual magnesium. To guarantee full nodulization of the main shaft, and considering actual production conditions and Si content, the residual Mg content is controlled between 0.04% and 0.055%.

The chemical composition of the main shaft is controlled as shown in Tab. 3.

Table 3. Chemical composition of the main shaft ($\omega B,\,\%)$

| С | Si | Mn | P | S | Mg |
|---------|-----------|-------|-------|-------|------------|
| 3.5~3.8 | 2.05~2.15 | ≤0.15 | ≤0.03 | ≤0.02 | 0.04~0.055 |

2.4 Simulation analysis of casting process

The 3D model of the main shaft is imported into casting simulation software for comprehensive analysis. The mesh is discretized into 15 million elements, with QT400-18 selected as the material. Shrinkage compensation efficiency is set to 90%, while the pouring temperature is maintained at 1340 °C for a duration of 200 seconds. The initial temperature of the sand mold is 20 °C. Thermal conductivity parameters are specified as follows: C600 for the interface between casting and sand mold, C2000 between sand mold and iron mold, and C3500 between iron mold and casting.

The filling process is a critical stage in casting, as an optimal filling can significantly reduce defects such as porosity, slag inclusion, and other impurities. Moreover, it provides favorable conditions for the subsequent

solidification process. The flow and temperature fields during the main shaft filling process are shown in Fig. 5. It is evident that throughout the filling process, molten metal enters the mold cavity from the bottom and fills it from bottom to top. The metal front remains nearly level, and the temperature distribution is uniform around the circumference, with no turbulence or splashing observed.

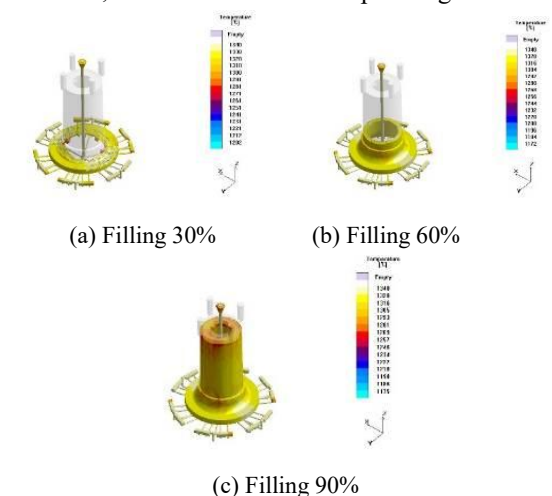


Fig. 5 : Filling process

The solidification process and liquid phase distribution are shown in Fig. 6, where the transparent areas represent the fully solidified phase, and the colored areas correspond to the liquid phase. The temperature field at the completion of filling serves as the initial condition for solidification. The thin-walled central section and the upper and lower end zones solidify first, followed by the top region, with the thickest bottom flange area solidifying last. The risers act to compensate for the insufficient shrinkage at the top, and once the shrinkage compensation is complete, the riser root solidifies, closing the channel and preventing molten metal from flowing back into the riser, thus avoiding shrinkage porosity defects.

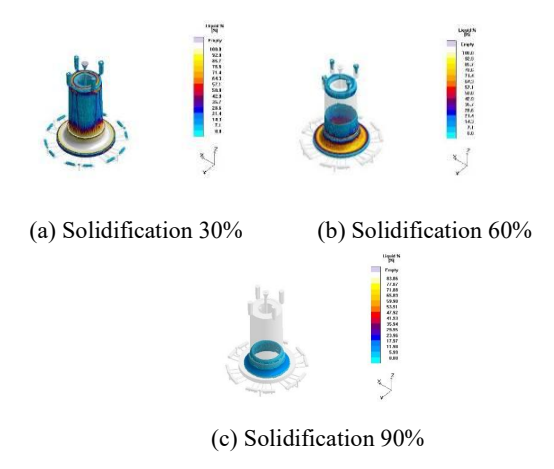


Fig. 6: Solidification process

Porosity analysis reveals that after solidification, significant shrinkage cavities appeared in the upper part of the riser, while the lower part and root of the riser remained relatively dense, indicating that the riser effectively compensated for the shrinkage of the casting. No more than 5% shrinkage porosity was observed in the casting, as shown in the fig. 7. Although the thick flange area, being the last to solidify, lacked risers and cold shuts, the absence of mold flexibility, the rapid cooling of the iron mold, which absorbs heat from the casting, and the combined effect of graphite expansion, all contributed to achieving internal density in the thick section. Based on this analysis, it can be concluded that the casting process is reasonable.

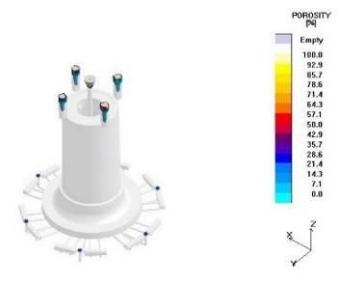


Fig. 7: Porosity criterion

3 Experiment and Validation

3.1 Control of the Melting Process

High-quality molten iron is the foundation for the internal quality and material properties of the casting, and obtaining high-quality molten iron is a prerequisite for effective nodulization. High-quality molten iron refers to ensuring the purity of the molten metal while maintaining the original quantity of the molten metal's core nuclei, allowing a substantial number of heterogeneous nuclei to be preserved. It also involves ensuring the appropriate chemical composition and pouring temperature of the molten iron.

High-carbon pig iron with low levels of Si, Mn, P, S, and trace elements such as Ti, Cr, Sn, Sb, and Pb is selected for the process. The scrap steel chosen contains low levels of alloying elements, specifically A3-grade scrap steel. The carburizing agent used is low in sulfur and easy to absorb, with a carbon absorption rate of no less than 90%. The amount of return material added during batching does not exceed 30%.

Considering the stability of the nodulization reaction and the characteristic of rare earth elements in reducing low-temperature impact toughness, a low-magnesium, low-rare-earth nodulizer is selected. The magnesium oxide content is required to be less than 0.8%, and the amount of nodulizer added is between 1.1% and 1.2%.

To improve inoculation anti-degradation properties and enhance the inoculation effect, Si-Ca (Ba) inoculant is used to increase the number of graphite nodules and improve nodulization grade. Barium content is appropriately increased, considering its role in preventing inoculation degradation. Additionally, considering the role of bismuth (Bi) in increasing the number of graphite nodules, a trace amount of Bi is added to the stream inoculant. The inoculant addition amount is between 0.6% and 0.7%.

The melting process is carried out using a medium-frequency induction furnace. A high current is applied for rapid melting to prevent the occurrence of cold charge, which can lead to local overheating of the molten metal, causing the disappearance of heterogenous nuclei and reducing the number of graphite nodules after nodulization, thus affecting the nodulization effect. When the molten metal temperature reaches 1400 - 1420° C, samples are taken for pre-treatment carbon-silicon analysis, and adjustments are made until the desired composition is achieved. Once the molten metal temperature reaches 1450 - 1480° C, slag is skimmed off for purification, and the molten metal is prepared for tapping.

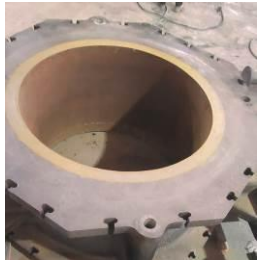
The nodulization process is carried out using an in-bag injection method, where the height-to-diameter ratio of the nodulization ladle is greater than 1.8. This design ensures better magnesium absorption and stability of the nodulization reaction. The bottom of the ladle is designed with a concave shape, with the concave area accounting for 2/5 of the total bottom area. The nodulizing agent is placed at the bottom of the ladle, and the inoculant is evenly spread on top, followed by a layer of thin steel sheets. During the nodulization treatment, the molten metal is injected towards the side of the ladle where no nodulizing agent has been placed, quickly filling the ladle with molten metal. At the final stage, the pouring speed is slowed. The nodulization reaction time is 70 to 120 seconds. After the nodulization process is complete, the molten metal is immediately transferred to the pouring area, where slag removal is carried out, followed by pouring. The entire process from the completion of nodulization to pouring must not exceed 18 minutes.

The inoculant addition procedure is as follows: 0.25% Si-Ba inoculant is added at the bottom of the nodulization ladle and evenly spread over the nodulizing agent; 0.15% high-silicon barium inoculant is used as a pre-treatment agent and placed at the location where the molten metal directly impacts the ladle bottom; the

remaining inoculant is added to the pouring trough during the pouring process, as a stream inoculant.

3.2 Production Trial

The sand covering process was completed using a custom-built sand-shooting machine. A special high-refractory membrane sand was selected for the process. Before sand shooting, the mold and iron mold were heated to a temperature of 180-200° C. The sand shooting pressure was set at 0.3-0.4 MPa, and the sand shooting time was controlled for 10-20 seconds. After a curing time of 200-300 seconds, the mold was removed. The iron mold after sand covering is shown in Fig. 8. The bottom box, top box, and core were all made using resin sand by manual molding, with the ceramic tubes for the pouring system embedded in the resin sand mold.





(a) Sand coating molding

(b) Molding box assembly





(c) Pouring

(d) Unboxing and cleaning

Fig. 8: Production process of the main shaft

Before closing the mold, all external molds and cores were coated with two layers of alcohol-based zirconium powder coating, followed by ignition to dry. Positioning pins were used for alignment, and the core was placed sequentially into the mold. During the core placement, the cavity dimensions in all four directions of the iron mold were checked and adjusted until the cavity dimensions were uniform. After the mold was closed, locking screws were used to secure all flanges of the iron mold. Electric shake-out pouring was employed with a pouring temperature of 1340 - 1350° C and a pouring time of 240 seconds. During pouring, a funnel was used for the continuous addition of the inoculant. After pouring, the mold was opened 48 hours later to retrieve the casting, which was then cleaned, ground, and shot-blasted.

3.3 Product Validation

The castings were visually inspected, and the surface was found to be clean with no sand adhesion. The flash thickness at the parting line did not exceed 1 mm, and the overall appearance consistency was good. The entire casting was subjected to ultrasonic testing according to GB/T 7233, and the results met the technical requirements for Level 2. Additionally, the surface was inspected using magnetic particle testing, revealing only slight localized defects, with no linear defects exceeding the allowed limits, thus satisfying the technical specifications. 3D scanning measurements were also carried out, and all dimensions of the casting met the precision requirements of GB/T 6414-CT9.

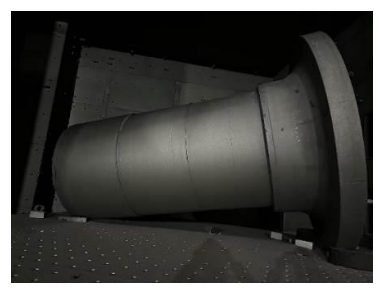


Fig. 9 : Condition of the wind power main shaft after shot blasting

Tensile and impact performance tests were conducted according to GB/T 228.1 and GB/T 229, and the results of the main shaft with cast test blocks are shown in Table 4. The test results indicate that all the sample properties meet the new material design specifications, with a substantial margin. Specifically, the yield strength margin exceeds 40 MPa, and the elongation at break margin exceeds 9%. The results of the two samples are closely consistent, with the tensile strength-to-yield strength ratio reaching 67%, demonstrating the high stability of the mechanical properties of the samples.

Table 4. Testing results of attached cast test blocks

| | TS | YS | Elanastian | AkV (-20°C)/J | |
|-----------------|-------|-------|----------------|-----------------|------------------|
| Grade | (MPa) | (MPa) | Elongation (%) | Single Value | Average Value |
| 1# | 419 | 284 | 21.0 | 12 | 1.1 |
| 2# | 424 | 286 | 22.5 | 11 10 | 11 |
| Avg | 421.5 | 285 | 21.75 | - | |
| Design Specs | 390 | 240 | 12.0 | 7 | 10 |

To investigate the mechanical properties of the main shaft body, tensile and impact tests were conducted on samples taken from the flange face and the small diameter end of the main shaft according to the technical requirements in the main shaft drawing. The sampling positions are shown in Fig. 10. Among the samples, 1#, 2#, 5#, and 6# were subjected to tensile and metallographic tests, while 3#, 4#, 7#, and 8# were subjected to impact tests. The tensile test results are shown in Table 5, and the impact test results are shown in Table 6. The test results indicate that the mechanical properties of the main shaft samples meet the performance requirements of the attached cast test bars.





Fig. 10 : Sample collection location diagram

Table 5. Body tensile test results

| Grade | TS (MPa) | YS (MPa) | Elongation (%) |
|-------|----------|----------|----------------|
| 1# | 422 | 286 | 18.0 |
| 2# | 419 | 282 | 22.5 |
| 5# | 411 | 278 | 21.5 |
| 6# | 410 | 279 | 13.0 |
| Avg | 415.5 | 281.25 | 18.75 |

Table 6. Body Impact Test Results

| | AkV(-20°C)/J | | | | | |
|-------|--------------|------------------|----|----|--|--|
| Grade | S | Average Value | | | | |
| 3# | 10 | 10 | 10 | 10 | | |
| 4# | 11 | 11 | 11 | 11 | | |
| 7# | 9 | 9 | 9 | 9 | | |
| 8# | 9 | 10 | 10 | 10 | | |
| Avg | - | - | - | 10 | | |

The metallographic images of samples 1#, 2#, 5#, and 6# are shown in Fig. 11. According to GB/T 9441 standards, the graphite particles are predominantly round, with good roundness, and the graphite size is rated at level 6-7. The spheroidization rate exceeds 92%. Additionally, after corrosion of the metallographic samples, the microstructure was examined, and the metallographic images are shown in Fig. 12. The ferrite content is over 95%, while the pearlite content is less than 5%.

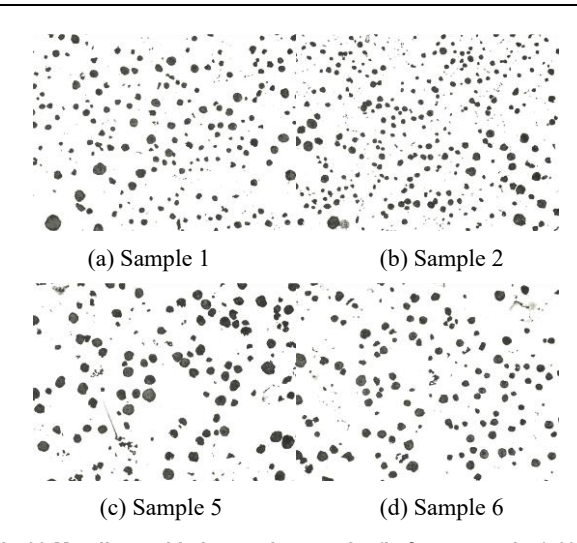


Fig.11:Metallographic inspection results (before corrosion) 100×

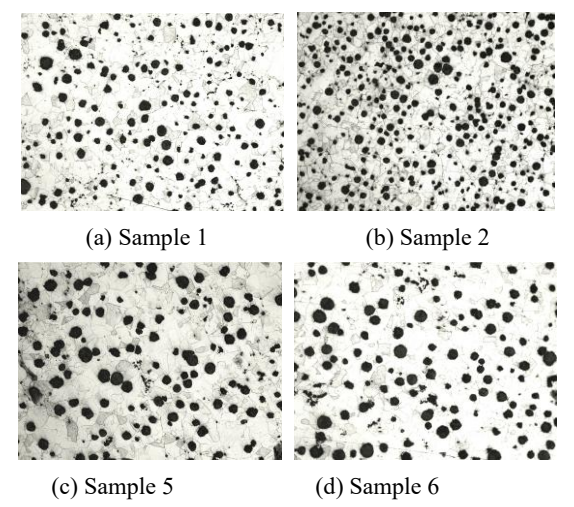


Fig. 12: Metallographic inspection results (after corrosion) 100×

4 Results Analysis

To thoroughly study the mechanical properties of the shaft body, samples were taken from the core regions of the top, middle, and bottom of the shaft, in accordance with the casting method used. The sampling locations are shown in Figure 13. Samples for tensile and impact tests were taken from the A and B ends, and samples for impact testing were taken from the C end. Specifically, 28 tensile samples and 32 impact samples were taken from the A end, 26 tensile samples and 32 impact samples from the B end, and 32 impact samples from the C end.

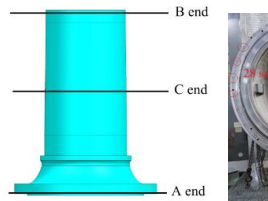
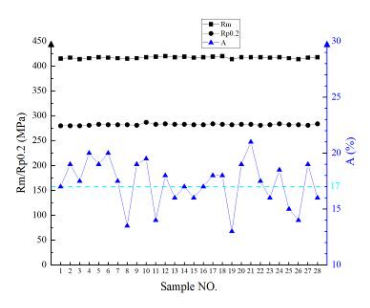




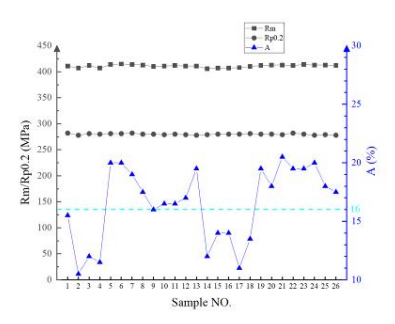


Fig. 13:Sampling Locations of Main Shaft Body

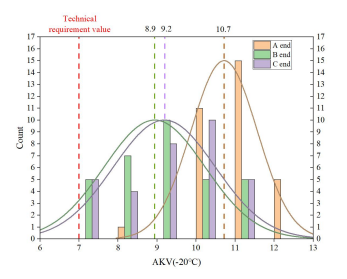
The test results are shown in Figure 14. From a circumferential perspective, all samples demonstrated a stable tensile strength exceeding 400 MPa, a yield strength around 280 MPa, and an average elongation after fracture of over 16%. The strength of the body samples met the requirements for the attached cast samples, with the yield strength surplus reaching over 40 MPa. Within the same cross-section, the tensile strength and yield strength data were very close, with only a few samples showing some dispersion in elongation after fracture, but all samples exhibited elongation greater than 10%. In terms of impact testing, the impact energy of all samples was above 7 J, with the average impact energy exceeding 8 J. The average impact energy at the A-end cross-section reached 10.7 J, nearly matching that of the attached cast samples. The variation in impact energy across different samples within the same cross-section was minimal. These results indicate that the material strength and impact toughness are essentially consistent across different locations on the same axial cross-section of the shaft.



(a) Tensile test of A



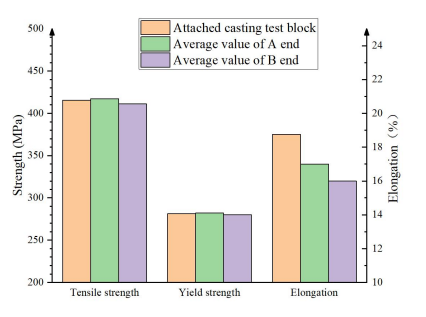
(b) Tensile test of B



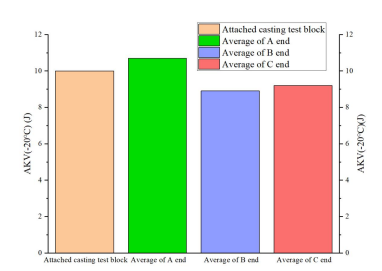
(c) Impact test of A, B, and C

Fig. 14:Statistical results of main shaft body samples

At the same time, the axial comparison of the A-end, B-end, and C-end test data was performed, as shown in Figure 15. It can be seen that the tensile strength, yield strength, and elongation after fracture of the A-end and B-end are very similar, with the A-end slightly higher than the B-end. The impact test results for the A-end, B-end, and C-end are also quite similar, with the A-end being the best, followed by the C-end, and the B-end coming last. Additionally, when comparing the body sample results with the attached cast sample, the tensile strength, yield strength, and impact toughness of the body samples are comparable to those of the attached cast samples, with the elongation after fracture being about 3% lower in the body samples. This demonstrates that the shaft exhibits good consistency in performance across its axial cross-sections, and the mechanical properties of the shaft body are comparable to those of the attached cast samples. Thus, the attached cast samples are fully representative of the mechanical performance of the shaft body.



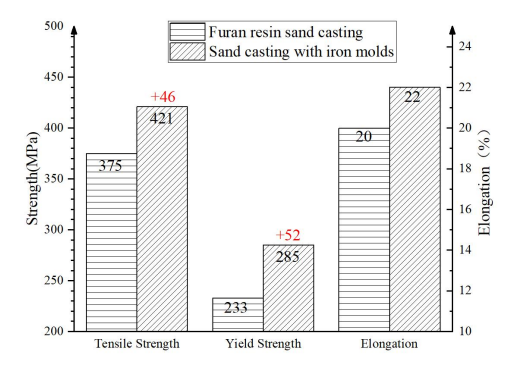
(a) Comparison of tensile test results



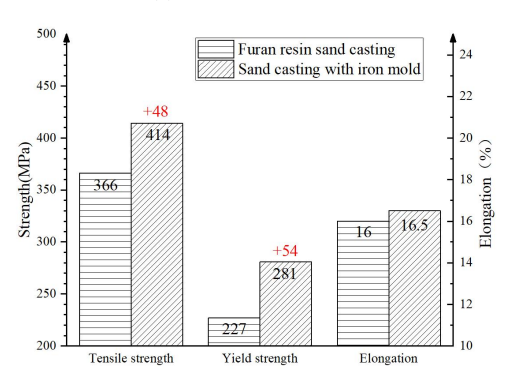
(b) Comparison of impact test results

Fig. 15:Performance comparison between main shaft body and cast-in test blocks

A comparison and analysis of the mechanical properties of the shaft produced using sand-coated iron mold casting versus the resin sand shaft from previous years is shown in Figure 16. It can be observed that, compared to the resin sand process, the sand-coated iron mold casting shaft achieves a significant increase in tensile strength and yield strength, with an improvement of over 40 MPa, while maintaining a slight improvement in elongation after fracture.



(a) Cast-in test block



(b) Main shaft sampling

Fig. 16:Performance comparison between sand-coated iron mold casting main shaft and resin sand main shaft

5 Conclusion

- (1) Enhanced Mechanical Properties of the Main Shaft: The use of sand-coated iron mold casting combined with the new material design led to a significant improvement in the mechanical properties of the wind turbine main shaft. The tensile strength and yield strength of the body samples were increased by over 40 MPa compared to conventional materials like QT400-18AL, while maintaining an elongation after fracture of over 16%. These improvements ensure the main shaft meets the stringent performance requirements for high-torque, low-temperature environments.
- (2) Consistent Mechanical Performance Across Axial Cross-Sections: The tensile strength, yield strength, and impact toughness of samples taken from different axial locations (A, B, and C ends) exhibited minimal variation, demonstrating the uniformity of the casting process. The average impact energy was above 7 J, with the A-end samples showing the highest values, indicating high consistency and reliability across the main shaft.
- (3) Superior Performance Compared to Resin Sand Casting: The main shaft produced using the sand-coated iron mold casting process exhibited a significant increase in tensile strength and yield strength over the resin sand castings, with improvements of over 40 MPa. This

indicates that the sand-coated iron mold casting method not only enhances mechanical performance but also provides a more reliable alternative to traditional casting methods for large, high-performance components like wind turbine main shafts.

Conflicts of interest:

The authors declare that they have no known competing financial interests or personal relationships that could have appeared to influence the work reported in this paper.

References

- [1] X R Yu, X Q Li. An Introduction to China National Standard "Wind Turbine Generator Unit, Spheroidal Graphite Cast Iron Castings" [J]. Modern Cast Iron 2009, 29(4):29-34.
- [2] L H Zheng, W X Tian. J J Sun, et al. Overview on Porosity Forming Mechanism of Spheroidal Graphite Iron [J]. China Foundry 2005(11):1063-1065
- [3] L Q Huang. Casting Technique of Sand-lined Iron-mold and Its Application [J]. China Foundry 1999(2):38-40
- [4] L Q Huang, D J Pan, Y H Shen. Sand-coated iron mold Casting and Its Applications [M]. Mechanical Industry Press, 2020.
- [5] B M Zhang. Handbook of Casting [M]. Mechanical Industry Press (1): 328.
- [6] I Riposan. M Chisamera, S Stan. Influencing factors on as-cast and heat treated 400-18 ductile iron grade characteristics [J]. China Foundry, 2007(4):400.